JOURNAL OF Applied Polymer SCIENCE

Cure Study of Epoxy Resin Reinforced with Multiwalled Carbon Nanotubes by Raman and Luminescence Spectroscopy

L. S.Cividanes,[1] D. D. Brunelli,[1] E. F. Antunes,[2] E. J. Corat,[2] K. K. Sakane,[3] G. P. Thim[1]

[1]Divisão de Ciências Fundamentais, Instituto Tecnológico de Aeronáutica (ITA), São José dos Campos, SP, Brazil

[2]Laboratório Associado de Sensores e Materiais, Instituto Nacional de Pesquisas Espaciais (INPE), São José dos Campos, SP, Brazil

[3]Instituto de Pesquisa e Desenvolvimento, Universidade do Vale do Paraíba (UNIVAP), São José dos Campos, SP, Brazil

Correspondence to: L. S.Cividanes (E-mail: lucianac@ita.br)

ABSTRACT: Carbon nanotubes (CNTs) were annealed at high temperature under vacuum, followed by a chemical treatment using acids and ethylenediamine. The presence of acid and amine chemical groups on CNT surface was confirmed by infrared spectra. The amount of iron remaining in the CNTs after the treatments was evaluated by thermogravimetry and by energy dispersion spectroscopy. The crystalline property of CNTs was evaluated by Raman spectroscopy, showing that the acid treatment performed after the thermal treatment did not damage the nanotubes walls. Micrographs showed that the most dispersed CNTs were obtained after the amine functionalization step. The curing process of the neat resin and composites was studied by Raman and Luminescence spectroscopies and both techniques showed similar results. The presence of CNTs, functionalized or not, increased the cure degree of the epoxy resin when the same cure time was used in the comparison. Nanocomposites synthesized with annealed CNT and acid-treated CNT had cure rates considerably higher at the beginning of the reaction. The difference in the cure rate was explained by means of the sample's homogeneity and the presence of chemical groups. © 2012 Wiley Periodicals, Inc. J. Appl. Polym. Sci. 000: 000–000, 2012

KEYWORDS: nanocomposites; resins; functionalization; curing; luminescence

Received 11 August 2011; accepted 30 March 2012; published online
DOI: 10.1002/app.37815

INTRODUCTION

Epoxy resins are thermoset materials with high performance, which are widely used in various industrial applications.[1,2] The addition of carbon nanotubes (CNTs) to the epoxy resin has been being used in recent years due to the extraordinary mechanical, electrical, and thermal properties of CNTs.[2] These nanocomposites have a number of interesting features and they have been being used in electronics and aeronautics industry.[3,4]

A common problem of CNTs/epoxy composites synthesis is the difficulty in dispersing CNTs in the epoxy resin. CNTs functionalization has been an effective way to prevent CNT agglomeration.[5] Some of the most common CNTs functionalizations are those that use acid and amine groups. Works[6–10] have shown that the mechanical properties of functionalized CNT/epoxy composites are better than nonfunctionalized CNT/epoxy ones. Some of these mechanical properties are: flexural strength, storage modulus, yield strength, and Young's modulus. Usually, amine-functionalized CNTs provide a higher reinforcing effect when compared with acid functionalized CNTs. Shen et al.[6] believe that amine-functionalized CNTs can easily integrate the epoxy matrix through covalent bonds between the amine groups of CNTs surface and the epoxy matrix. This would explain the further strengthening of amine-functionalized CNTs when compared with acid functionalized CNTs.

The nanocomposites final properties significantly depend on the curing conditions.[11–15] The curing studies of epoxy resin in the presence of CNT are very important to the design, analysis, and optimization of the material manufacturing, as its addition to epoxy resin influences the curing process.[11–13] Many recent studies have investigated the curing process of CNT/epoxy nanocomposites. Puglia et al. showed that the incorporation of single-walled CNTs (SWCNTs) to epoxy resin accelerates the epoxy curing reaction. This effect was explained by the extremely high SWCNTs thermal conductivity.[3] Tao et al.[4] showed that SWCNTs can initiate cure at lower temperatures, but the overall curing process was slower. Yang et al.[16] showed that the nonfunctionalized multiwalled CNT (MWCNT) has the effect of slowing the curing reaction of epoxy resin, whereas amine-

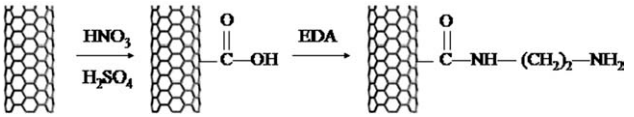

Figure 1. Scheme of CNT functionalization.

functionalized MWCNTs has the effect of accelerating the cure. Abdalla et al.[17] showed that carboxyl and fluorine have modified MWCNTs cure degree and glass transition temperature similar to that of neat resin, but the enthalpy of curing was lower for the nanocomposites than for the neat resin. Zhengping et al. prepared samples using a weight ratio of 1% of MWCNTs/epoxy resin and they observed that: (i) the curing heat of the amine-functionalized CNTs and epoxy resin system was higher than that for the neat resin; (ii) the enthalpy of curing for nonfunctionalized CNTs and epoxy resin system was lower than that for the neat resin; (iii) using a higher MWCNT concentration (2%), the curing enthalpy for both composites was lower compared with that one obtained for the neat resin.[18]

As can be seen, it is unclear how the CNTs, functionalized or not, react with the epoxy resin and how it affects the nanocomposite curing process. Moreover, the study of the influence of CNT in the epoxy curing has been performed in the literature mainly by differential scanning calorimetry (DSC). Although luminescence spectroscopy, which is a nondestructive and high sensitivity technique and has been successfully used for monitoring the curing process of several polymers,[19,20] has not yet been used to study the curing process of this nanocomposite. Therefore, this study aims to investigate the influence of functionalized and nonfunctionalized MWCNTs on the curing reaction of epoxy resin by luminescence spectroscopy, correlating these results with those obtained by Raman spectroscopy, which is a more conventional technique.

EXPERIMENTAL PROCEDURES

Preparation of Purified and Functionalized Carbon Nanotubes

MWCNTs were synthesized by pyrolysis of camphor mixed with 16% of ferrocene (chemical vapor deposition method) and provided by the Laboratório Associado de Sensores e Materiais from Instituto Nacional de Pesquisas Espaciais, Brazil. Nanotubes have diameters from 60 to 100 nm and length from 500 to 600 μm, according to supplier's specification. CNTs were pre-purified by a heat treatment at 1800°C for 3 h at 10^{-2} Pa to eliminate iron and other impurities.[21,22] The presence of the iron-containing phases in the MWCNT samples are inherent in the production process, due to iron is used as a catalyst. The further purification was performed with subsequent acid treatment. Besides the fact that the acid treatment promotes the purification of CNTs, it also aims to functionalize the nanotubes with carboxylic groups.

A portion of CNTs annealed at 1800°C was treated with a mixture of sulfuric acid (H_2SO_4, 98%, Merck, 90 mL) and nitric acid (HNO_3, 70%, Vetec, 30 mL) (3 : 1 by volume) in an ultrasonicator bath with power of 125 W for 5 h at room temperature. After that, distilled water was added and the mixture was sonicated for another 1 h. After this process, the oxidized CNTs were obtained by a filtering process using a cellulose nitrate filter membrane (0.45 μm pore size) with the help of a vacuum pump. Bidistilled water was added to CNT until the filtered water reached a neutral pH. Samples were dried in a vacuum oven at 40°C for 16 h.

For the functionalization with amine groups, part of the oxidized nanotubes (0.3 g) were dispersed in ethylenediamine ($C_2H_4(NH_2)_2$, EDA, 175 mL). The mixture was dispersed using an ultrasonicator bath for 1 h. Then, the mixture was kept under magnetic stirring and heated at 100°C for 4 days under reflux. After that, the CNTs were vacuum filtered using a 0.45-μm polytetrafluoroethylene membrane. Then, the CNTs were washed with ethanol (Synth) to remove EDA excess. The sample was dried in a vacuum oven at 40°C for 16 h. Figure 1 shows a scheme of the CNT functionalization and Figure 2 shows the nomenclature of the purified and functionalized CNTs.

Preparation of Nanocomposites and Neat Resin

The neat resin (ResCNT-0) and nanocomposites (ResCNT-An, ResCNT-Ac, and ResCNT-Am) were synthesized with Araldite GY 260 epoxy resin, based on diglycidyl ether of bisphenol A (DGEBA) and with Aradur 972 hardener, based on diaminodiphenylmethane, both manufactured by Huntsman. The nanocomposites were synthesized with 0.2 wt % of nanotubes.

CNTs were dispersed in acetone into an ultrasonicator bath for 30 min and then they were added to the epoxy resin. CNT and the epoxy resin were mixed using a tip sonication (UP 200S, Hielscher, 200 W) at 65°C. The mixture was degassed at 80°C for 24 h. After that, the hardener was added while being heated at 85–90°C, with a resin-to-hardener weight ratio of 100 : 27. The composite resin was cast into preheated mould of silicone.

Characterization Methods

FTIR was used to study the presence of chemical groups on the CNT surface. Infrared spectra were recorded in a Perkin–Elmer Spotlight 400 FT-IR and Imaging System, in the range of 4000–850 cm^{-1}, using a resolution of 4 cm^{-1}, 32 scans and KBr pellet method.

Raman spectra were used to show the graphitic ordering before and after the thermal annealing and functionalization. The spectra were registered using a Renishaw 2000 Micro-Raman, equipped with argon laser (514.5 nm), in the range of 1000–2000 cm^{-1}.

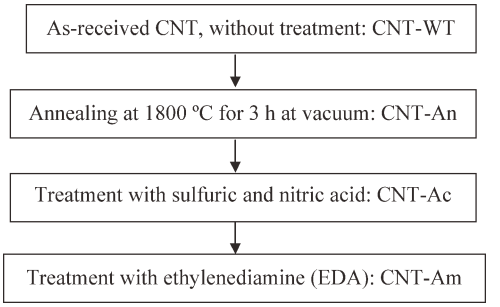

Figure 2. CNTs nomenclature.

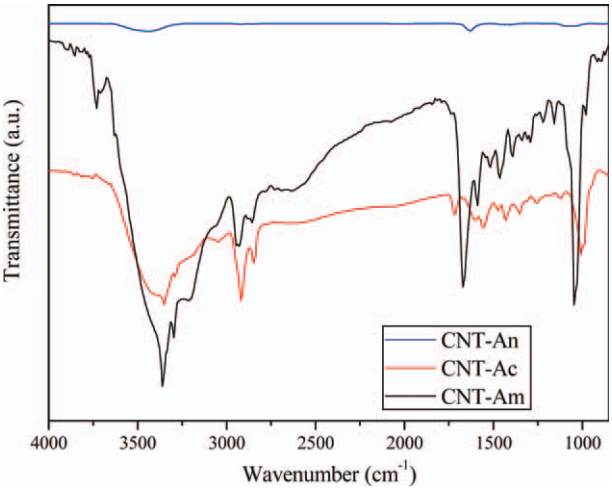

Figure 3. FTIR spectra of purified and functionalized CNTs. [Color figure can be viewed in the online issue, which is available at wileyonlinelibrary.com.]

The amount of iron, remaining in the CNTs after the treatments, was evaluated by thermogravimetry/derivative thermogravimetry (TGA/DTG) and by energy dispersion spectroscopy (EDS) in a EVO MA10 (Zeiss) scanning electron microscope (SEM). CNTs samples (10 mg) were analyzed in a TGA 7 HT, PerkinElmer, from 25 to 1000°C, at 10°C/min, in synthetic air. The microstructure of CNTs at lower magnifications was recorded in a microscope JEOL JSM-5310 (SEM). CNTs microstructure at higher magnification and the morphology of the cryogenically fractured surfaces of composites were observed using a field emission gun-scanning electron microscope (Philips FEG-SEM).

The curing process was studied by luminescence and Raman spectroscopies. Samples of neat resin and nanocomposites subjected to two curing times (curing at 120°C for 0 and 2 h after the precuring at 80°C for 1 h) were analyzed by Raman spectroscopy. The spectra were registered using a Renishaw 2000 Micro-Raman, equipped with argon laser (514.5 nm), in the range of 500–3500 cm^{-1}. Samples of neat resin and nanocomposites precured at 80°C for 1 h and after cured at 120°C for different times (0, 30, 60, 90, 120, 180, 240, 300, 360, 600, and 1080 min) were subjected to luminescence spectroscopy, using a steady-state luminescence spectrometer (FS920—Edinburgh Analytical Instruments), equipped with a xenon arc lamp 450 W (Osram). The excitation and emission wavelengths were 300 and 350 nm, respectively.

RESULTS AND DISCUSSION

Characterization of Carbon Nanotubes

Figure 3 shows the FTIR spectra of CNTs subjected only to the annealing treatment and also those subjected to the chemical treatments. The assignments of the infrared peaks are shown in the Table I.[8,10,23–30]

The FTIR spectrum of the sample CNT-Ac shows the following bands and peaks: at 1723 cm^{-1} because of the C=O stretching vibration in the carboxylic acid group,[10,23,26,27] at 1600 cm^{-1} related to the —COO^- asymmetric stretching,[23] at 1430 cm^{-1} which can be attributed to the O—H bending of the carboxylic group[28] and at 1007 cm^{-1} due to the —C—O stretching in primary alcohol.[8,23] These peaks indicate that the acid treatment of CNT successfully introduced COOH, OH and C=O groups on the nanotube walls. FTIR spectra of the sample CNT-Am shows that the band at 1723 cm^{-1} almost disappears completely, and a new peak appears at 1670 cm^{-1}, which corresponds to the amide carbonyl (C=O) stretching, making it possible to conclude that the —OH chemical group of the carboxylic acid was turned into an amide group. The FTIR spectra of the sample CNT-Am shows bands at 3728 cm^{-1} because of the —NH stretching,[23] at 1587 cm^{-1} due to the N—H in-plane bending,[8,24,26,27,30] and at 1220 and 1047 cm^{-1}, which are assigned to the C—N

Table I. Assignments of the Infrared Peaks Purified and Functionalized CNTs

Sample	Peak (cm^{-1})	Interpretation
CNT-An	3445	OH stretching of the carboxylic (COOH) group[23–25]
	1630	Overlapped vibrations of double bonds C=C and carbonyl groups C=O[26]
CNT-Ac	3351, 3289	OH stretching of the carboxylic (COOH) group[23–25]
	2918, 2847	—CH stretching[23,25]
	1722	C=O stretching of the carboxylic (COOH) group[10,23,26,27]
	1600	—COO^- asymmetric stretching[23]
	1554	Vibration of carbon skeleton (C=C) of the CNTs[27–29]
	1430	O—H bending of the carboxylic (COOH) group[28]
	1007	—C—O stretching in primary alcohol[8,23]
CNT-Am	3728	—NH stretching[23]
	3360, 3296	OH stretching of the carboxylic (COOH) group[23–25]
	2945, 2929, 2856	—CH stretching[23,25]
	1670	C=O stretching of the amide carbonyl[6,23,26,30]
	1587	N—H in-plane bending[8,24,26,27,30]
	1518	Vibration of carbon skeleton (C=C) of the CNTs[27–29]
	1220, 1047	C—N stretching[8,26,30]

Applied Polymer SCIENCE

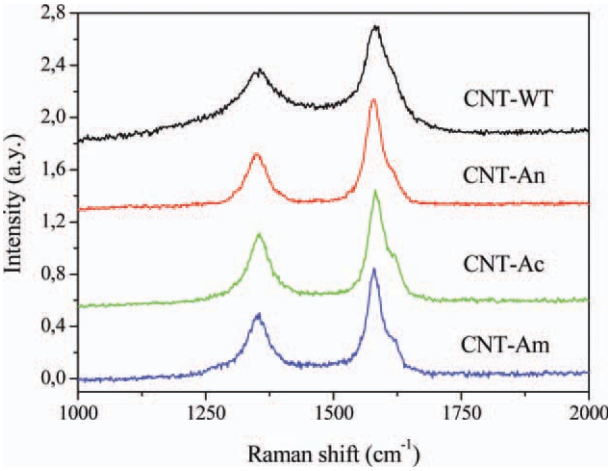

Figure 4. Raman spectra of samples CNT-WT, CNT-An, CNT-Ac, and CNT-Am. [Color figure can be viewed in the online issue, which is available at wileyonlinelibrary.com.]

stretching.[8,26,30] These bands indicate that the carboxylic groups present on the CNT surface were successfully modified by amine.

Figure 4 shows Raman spectra of samples CNT-WT, CNT-An, CNT-Ac, and CNT-Am. Figure 4 clearly shows two bands in each Raman spectrum: in 1350 and 1580 cm^{-1}, besides a shoulder at near 1620 cm^{-1}. These three bands are related to D, G, and D′ bands of CNT, respectively. These bands are characteristic of CNTs multiple walls,[31–33] and D band is attributed to the presence of disordered structures, such as defective CNT and noncrystalline carbon. Figure 4 shows that there is practically no shift in wavelength in relation to CNT treatments. However, the intensity and width of the peaks depend to each treatment. The crystallinity of a carbonaceous material can be determined by the ratio of the intensity of G and D bands, as well as the full width at half height of G band. A carbonaceous material constituted of smaller defect number shows higher values of the ratio between G and D band, as well as smaller width at half height of G band. Table II shows the ratio values of G and D bands, and full width at half height of G band. Table II shows that the ratio of G and D bands is not strongly dependent on CNT treatments, and the sample CNT-An had the lowest amount of defects (higher ratio of G/D bands). One can observe a higher value of the width at half height of G band for CNT-WT in relation to thermal treated samples. That is, CNT samples treated at 1800°C (CNT-An, CNT-Ac, and CNT-Am) show higher crystallinity and lower amounts of defects. Thus, the

Table II. Ratio Values of G and D Bands and Full Width at Half Height of G Band for Samples CNT-WT, CNT-An, CNT-Ac, and CNT-Am

CNT sample	Ratio G/D bands	Full width at half height of G band
CNT-WT	1.7	65
CNT-An	2.0	36
CNT-Ac	1.7	38
CNT-Am	1.8	37

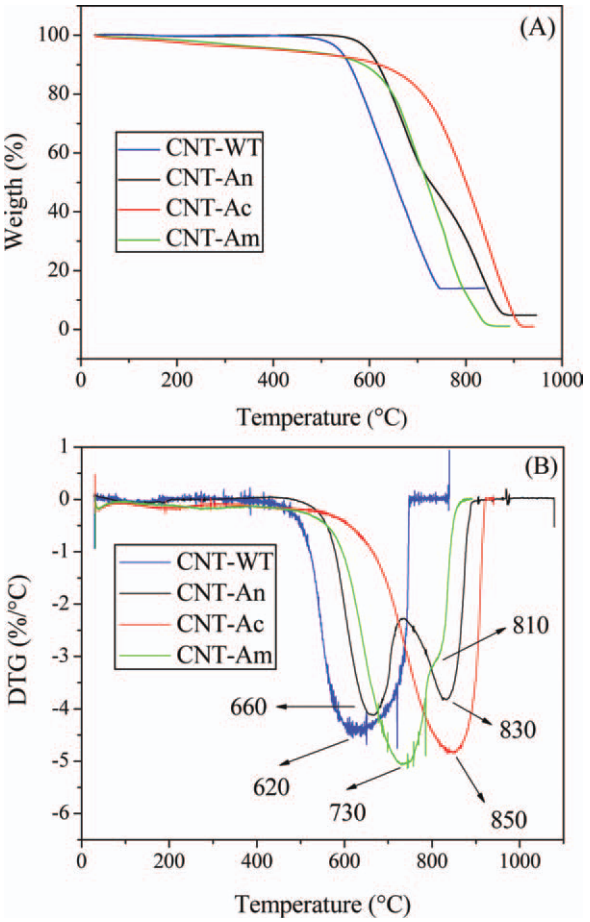

Figure 5. TGA (A) and DTG (B) curves for samples CNT-WT, CNT-An, CNT-Ac, and CNT-Am. [Color figure can be viewed in the online issue, which is available at wileyonlinelibrary.com.]

nonthermal treated sample (CNT-WT) showed a higher number of defects. Other works[21,22] has already shown that heat treatment at high temperatures is effective for elimination of preexisting defects in the CNT structure, and that the acid treatment eventually damages the CNT walls. However, the acid treatment, which was performed in this work after the heat treatment, did not damage the nanotubes walls. This can be explained by the defect elimination performed by the heat treatment in all MWCNT walls. However, reminding that MWCNT is constituted by several concentric walls, the acid treatment links carboxylic groups in the last MWCNT wall. Therefore, the acid treatment can only damage the most external wall.

The thermal behavior of nanotubes before and after the treatments, under oxidizing atmosphere, was studied by TGA/DTG (Figure 5). Figure 5A shows the decomposition of organic groups attached to CNT-Ac and CNT-Am until about 450°C. Other authors showed that organic groups covalently attached to CNTs were thermally stripped off in the temperature range from 250 to 500°C.[34] Samples CNT-WT and CNT-An show no mass loss at this temperature because there is virtually no organic group attached to the wall of the nonfunctionalized CNTs. Above this temperature, oxidation begins to occur at the

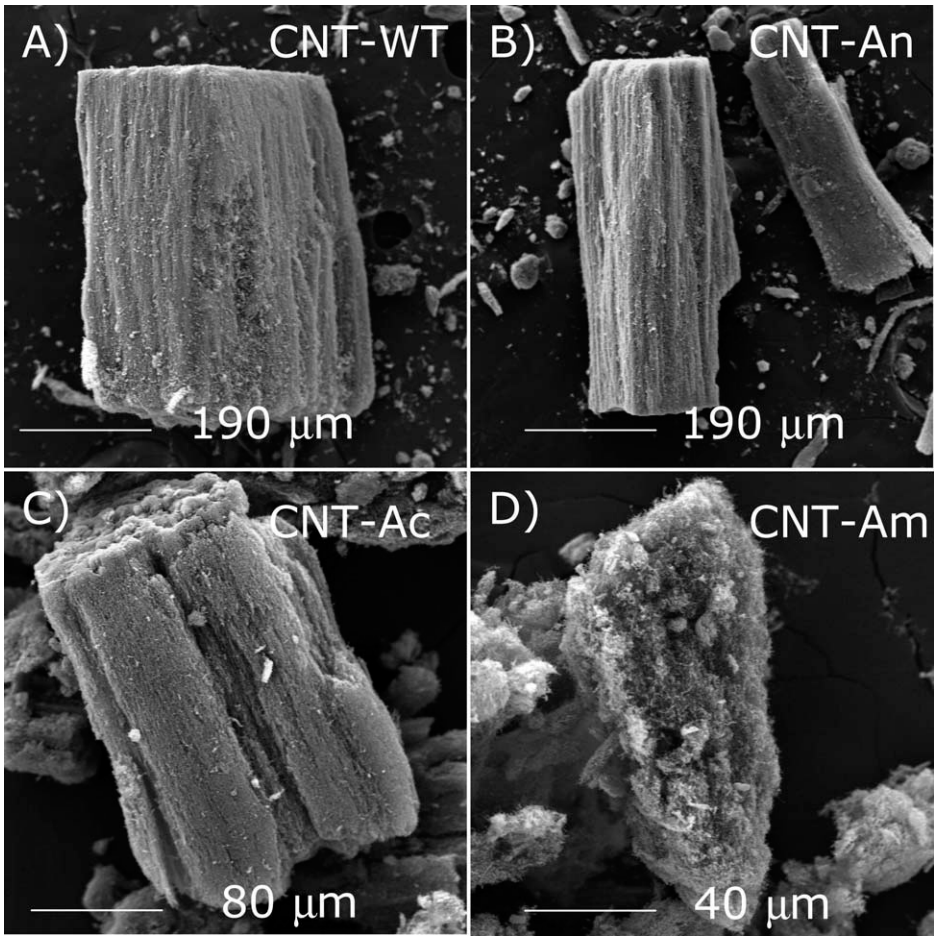

Figure 6. SEM micrographs of samples CNT-WT, CNT-An, CNT-Ac, and CNT-Am at lower magnifications.

carbon of the CNTs. The residual mass for CNT-WT, CNT-An, CNT-Ac, and CNT-Am were 14%, 4.8%, 1%, and 1%, respectively. The residual mass is mainly iron oxide.[22] According Huang et al.,[21] there is no good method by which the purity of CNT can be directly evaluated. Then, some authors have used TGA analysis to evaluate the amount of metal and metal oxide contents.[21,22] The residual mass results of this work indicated that the thermal annealing eliminated about 9.2% of the CNT impurities, and the subsequent acid treatment removed other 3.8% of the impurities that the heat treatment was not able to eliminate. EDS results showed no significant amount of iron in the samples CNT-An and CNT-Ac because of EDS analysis is not very accurate for determining the iron amount of CNTs. However, TGA analysis showed the presence of a residual mass in the samples CNT-An (4.8%) and CNT-Ac (1%). However, the low value (only 1%) of the residual in the sample CNT-Ac shows that the heat treatment followed by the acid treatment was very effective for the CNT purification, without damaging the structure of the nanotubes , which was already shown by Raman spectroscopy.

Besides that, Figure 5(A) shows a shift of the TGA curves of samples CNT-An, CNT-Ac, and CNT-Am to the right (after 550°C) compared to TGA curve of sample CNT-WT, indicating an increase in temperature required for oxidation. DTG curves from Figure 5(B) also show that the oxidation peaks of the samples CNT-An, CNT-Ac, and CNT-Am appear at temperatures higher than the sample CNT-WT. Therefore, the thermal stability of CNTs was improved with the annealing and chemical treatments. DTG curves also show that the reaction between CNTs and oxygen occurs in one step for samples CNT-WT and CNT-Ac, and in two steps for samples CNT-An and CNT-Am. The oxidation peak for the sample CNT-WT occurs at 620°C, whereas CNT-An has oxidation peaks at 660 and 830°C. For samples CNT-Ac, the oxidation peak occurs at 850°C, whereas the samples CNT-Am have oxidation peaks at 730 and 810°C (shoulder in DTG curve). The thermal annealing improved the structure of the sample CNT-An, because part of its material starts to oxidize at higher temperatures, at around 800°C. However, disordered or amorphous carbons, which tend to be oxidized at around 500°C, are still present.[34] This low oxidation temperature occurs because of the large number of active sites in the CNT structure or the lower activation energy for its oxidation.[34] The temperature oxidation of the sample CNT-Ac (850°C) is higher than the two peaks of sample CNT-An (660 and 830°C) as a result of an increase in the thermal stability, as the acid treatment may have destroyed the disordered or amorphous carbons of the CNT structure. Amine treatment slightly decreased the thermal stability on the sample CNT-Ac, but

Applied Polymer SCIENCE

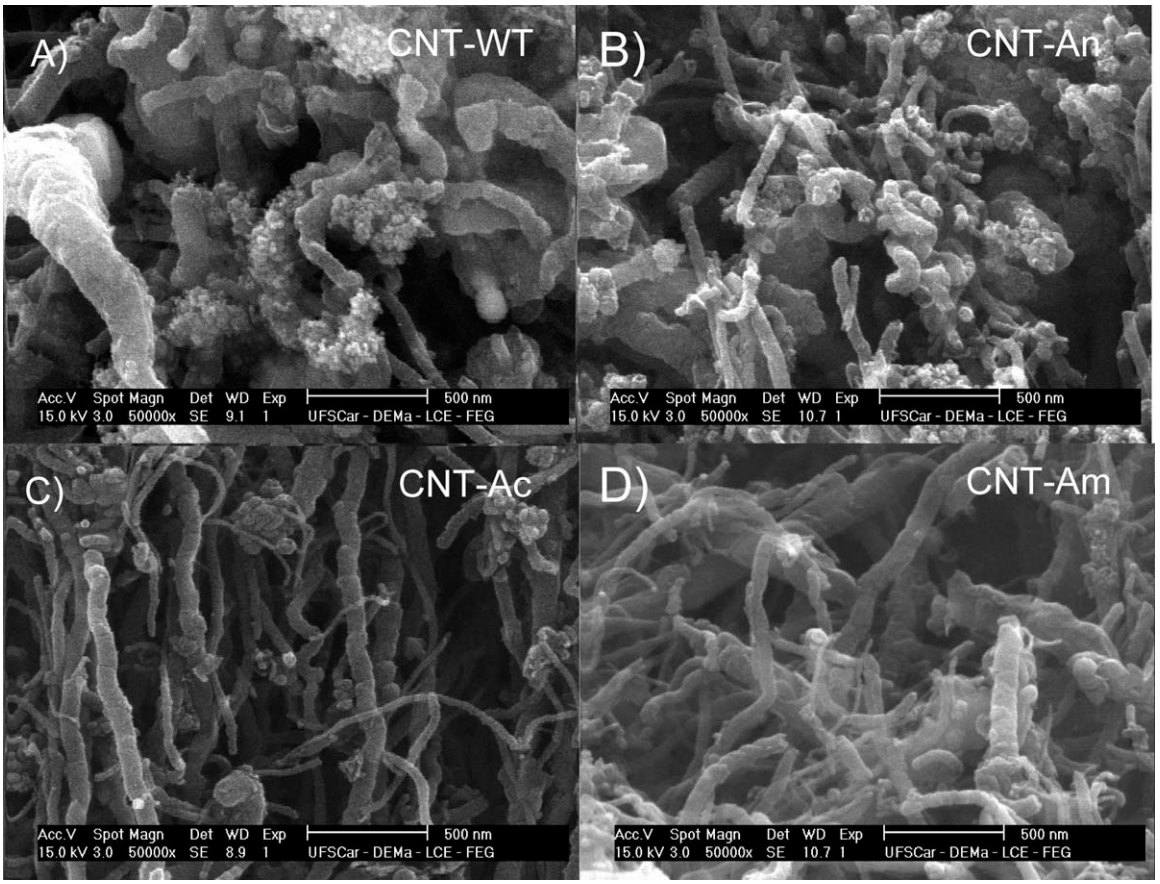

Figure 7. SEM micrographs of samples CNT-WT, CNT-An, CNT-Ac, and CNT-Am at higher magnifications.

sample CNT-Am was still more stable than sample CNT-WT. The treatment with EDA, by removing OH groups from the CNTs surface, may have caused some defects in their walls.

The microstructure of CNTs at lower magnifications are shown in Figure 6. The cylindrical figures in the center of the images are clusters of aligned CNTs. Figures 5(B) and 6(A) show that the nanotubes of samples CNT-WT and CNT-An were about 500 μm in length, but the length decreased to values about 250 [Figure 6(C)] and 150 [Figure 6(D)] μm after acid and amine treatment. Figure 6(A,B) show that CNT-WT and CNT-An have the smoothest surfaces. Figure 6(C) shows nanotubes with surfaces rougher than the two first ones, whereas Figure 6(D) shows nanotubes with the roughest surface. These textural properties of the CNTs are due to the presence of the functional groups added on the CNTs surface. Furthermore, Figure 6(D) also shows a shift in the orientation of the nanotubes in sample CNT-Am, which are no longer so aligned to each other, like in samples CNT-WT, CNT-An, and CNT-Ac [Figure 6(A–C)].

The micrographs of Figure 7 shows images of CNTs at higher magnifications. These micrographs show that the diameter of CNTs varies from 30 to 100 nm. The characteristic shapes of CNTs, which are tubular structures, are composed of a small diameter and a long length. The CNTs structures related to samples CNT-WT and CNT-An are not clearly seen in Figure 7(A,B), possibly because impurities such as amorphous carbon and iron cover the nonfunctionalized nanotubes. The presence of these impurities has already been predicted in the EDS and TGA studies, which were showed before. However, the structures of CNTs can be clearly seen in the micrographs of Figure 7(C,D), related to samples CNT-Ac and CNT-Am. Figure 7(C), and Figure 6(C) shows that nanotubes in the sample CNT-Ac are aligned in a parallel way with one other. That is, they have the same orientation, and so they are less dispersed. However, as shown in Figure 6(D), Figure 7(D) also shows that nanotubes in the sample CNT-Am are not aligned to each other, what creates a higher dispersion of nanotubes in relation to sample CNT-Ac.

Figure 8 shows the micrographs of the cryogenically fractured surfaces of nanocomposites. Figure 8(B,C) show the nonuniform distribution of CNTs in the nanocomposite ResCNT-An, as can be seen by the presence of a CNT agglomerate. Besides that, the adhesion between CNT and epoxy resin was poor, as many CNTs were pulled out of the matrix rather than broken. Figure 8(D) shows better uniformity and nanotube distribution in the matrix of sample ResCNT-Ac compared with samples ResCNT-An, but Figure 8(E), which is also related to sample ResCNT-Ac, shows the presence of a CNT agglomerate. Both Figure 8(D,E) show better interfacial bonding between CNT-Ac and the polymer resin than the other two samples, as CNTs are broken instead of pulled out. Therefore, acid treatment

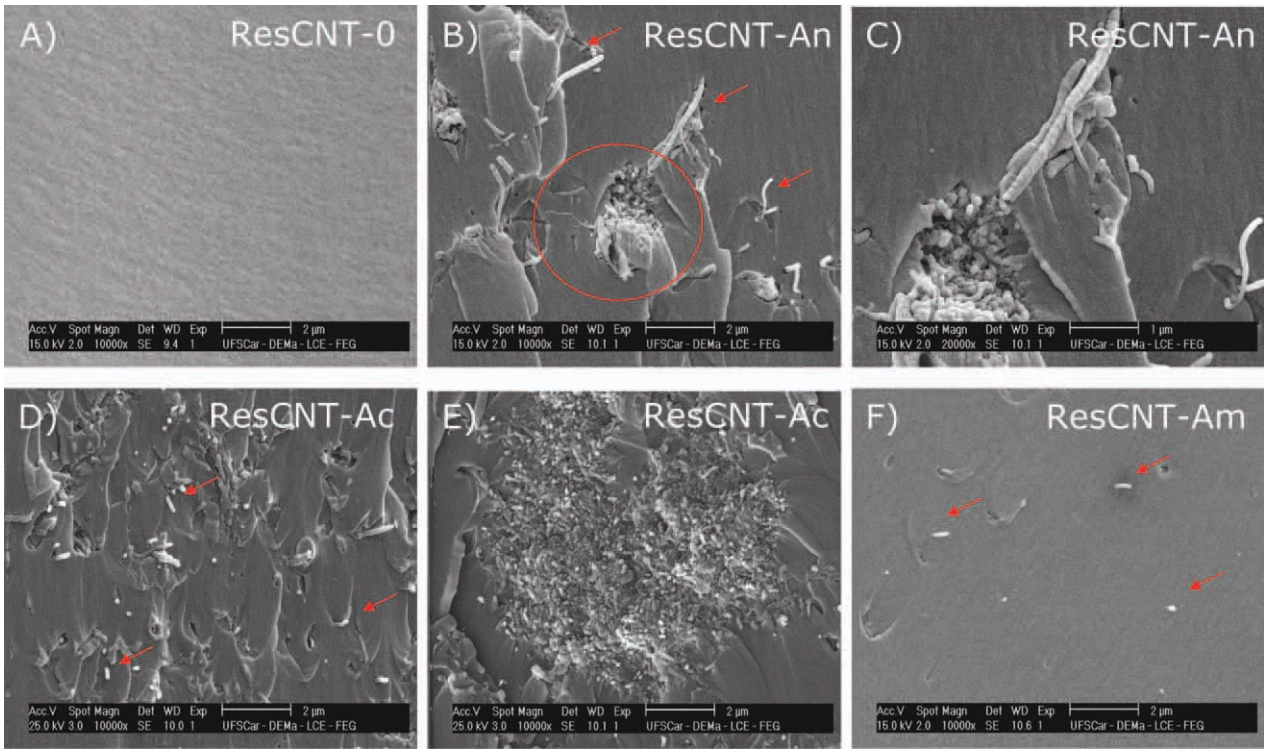

Figure 8. SEM micrographs of the cryogenically fractured surfaces of samples ResCNT-0, ResCNT-An, ResCNT-Ac, and ResCNT-Am. [Color figure can be viewed in the online issue, which is available at wileyonlinelibrary.com.]

improved adhesion between CNT and resin, and also promoted a little improvement in dispersion, although there was still the formation of agglomerates. Figure 8(F) shows a good distribution of CNTs in the matrix, and a good adhesion between CNT and epoxy, as can be seen by the small number of nanotubes present in the image and its small size. This indicates that this sample is the most homogeneous of all, and that CNT-Am has a better interfacial bonding between CNT and resin. The lack of organization of nanotubes that was observed for sample CNT-Am in Figure 6(D) may has created a less compact structure. This structure can promoted a better dispersion of CNTs in epoxy resin, as was also shown by Meng et al.[7]

Study of Curing Process

Raman spectroscopy was applied to samples submitted to the precured sample at 80°C for 1 h, and to samples submitted to cure at 120°C for 2 h (these last were previously precured at 80°C for 1 h). All Raman spectra (Figure 9 shows the spectra for sample ResCNT-0 before and after subtracting the baseline) showed the same peaks, only changing the intensity and the baseline to be subtracted.

Raman spectra show several peaks that refer to the disubstituted aromatic rings stretch of the epoxy resin. These peaks have different intensities and appear at 640, 805, 1109, 1184, 1450, and 1610 cm^{-1}. The more intense and better defined peak occurs at 1610 cm^{-1}, which is related to the strong stretching of aromatic ring C=C. This peak can be taken as a standard peak for the normalization of the spectra to determine the cure degree, as its intensity does not vary with the cure degree. Figure 9 also show: (i) characteristic peaks of the epoxy ring at 1260 cm^{-1} related to the epoxy ring breathing and at 830 cm^{-1} associated to the symmetric deformation of the epoxy ring; (ii) CH_2 stretching vibration that occurs at 2932 cm^{-1}; (iii) stretching of the C—H in epoxy ring that occurs at 3065 cm^{-1}.[35,36] The later peak can be used to control the cure degree, as its intensity decreases as the sample is cured due to the epoxy ring opening.

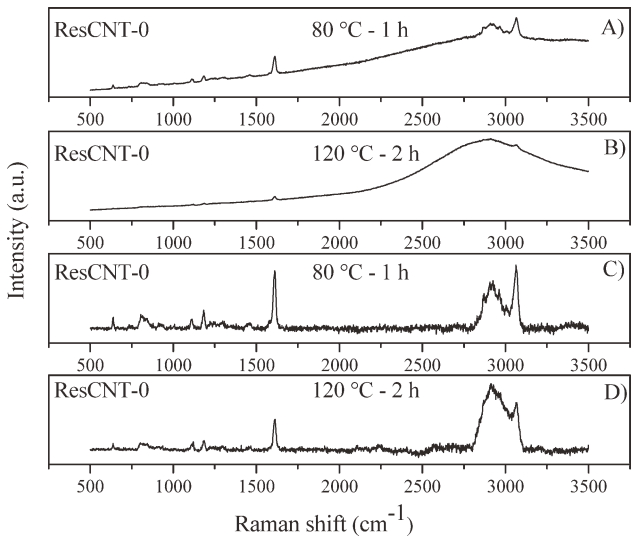

Figure 9. Raman spectra for sample ResCNT-0 precured at 80°C for 1 h and cured at 120°C for 2 hours after the precuring; A) and B) spectra before subtracting the baseline, C) and D) spectra after subtracting the baseline.

Table III. I_{1610}/I_{3065} for Samples ResCNT-0, ResCNT-An, ResCNT-Ac, and ResCNT-Am Precured at 80°C for 1 h and Cured at 120°C for 2 h

Sample	Cure at 80°C—1 h	Cure at 120°C—2 h
	(I_{1610}/I_{3065})	(I_{1610}/I_{3065})
ResCNT-0	0.96	0.68
ResCNT-An	0.98	0.97
ResCNT-Ac	0.98	0.93
ResCNT-Am	0.95	0.87

Thus, taking the peak to 1610 cm^{-1} as a standard for the normalization of the spectra, we can calculate the ratio (I_{1610}/I_{3065}) between the peak intensity at 1610 cm^{-1} by the intensity of the peak at 3065 cm^{-1}. This ratio is not the cure degree, because here we have just two sets of time/temperature, but it is related to the cure degree, that is, the cure degree increases when this ratio also increases. Table III shows the values for this ratio for samples ResCNT-0, ResCNT-An, ResCNT-Ac, and ResCNT-Am precured at 80°C for 1 h and cured at 120°C for 2 h after precuring.

A comparison between the values of Table III, for a same sample cured for different time/temperature, is a complicated task due to the different background effects in the Raman spectra obtained from samples treated at 80 and 120°C. This is because of the presence of luminescence activities of the system GY 260 epoxy resin/ Aradur 972 hardener, mainly in the region of peaks around 3000 cm^{-1}, as one can see from Figure 9(A,B). Each sample has a particular background effect associated with its set time/temperature of curing. Figures 9(A,B) show how the baselines to be subtracted depend on the curing temperatures. However, different samples cured by the same time/temperature have similar background effects because they have similar luminescence. Therefore, the intensity of the peaks in 1610 and 3065 cm^{-1} can be compared with samples cured at the same temperature and time, as the baselines to be subtracted are quite similar.

One can see in the Table III that the ratio values of the peaks 1610 and 3065 cm^{-1} for all samples cured at 80°C for 1 h are very close. Table III also shows that nanocomposite samples cured at 120°C for 2 h have considerably higher cure degree than the neat resin. In addition, between the nanocomposite samples, the cure degree is lower for sample ResCNT-Am, followed by sample ResCNT-Ac, and the sample with the highest cure degree is ResCNT-An.

Samples of neat epoxy resin and nanocomposites cured for different time periods at 120°C were subjected to luminescence spectroscopy. All emission spectra (Figure 10 shows the spectra for sample ResCNT-0) show only one peak around 350 nm. This peak refers to the epoxy ring of DGEBA, and so, the intensity of this peak has a tendency to reduce as the curing takes place. Then, a curve of cure degree (α), defined by eq. (1), can be obtained:

$$\alpha = \frac{I_t - I_i}{I_f - I_i} \quad (1)$$

where I_i means the intensity of the emission peak obtained from the studied sample after precure at 80°C for 1 h; I_f means the intensity of the emission peak obtained using the studied sample after cure at 120°C for 1080 min; I_t is the intensity of the emission peak obtained using the studied sample after thermal treatment at 120°C for a given period of time (t).

Figure 11 shows the curves of cure degree in function of time. The squares are the experimental points and the line is the fitting. Figure 12 shows all curves together for better comparison. Figures 11 and 12 show the curves of cure degree as a function of time. The nanocomposites showed higher cure rate compared to the neat resin throughout the reaction. The final cure degree was about 1 for sample ResCNT-An and 0.98 for samples ResCNT-Ac and ResCNT-Am. However, the sample ResCNT-0 achieved a cure degree considerably lower: 0.93. This dependence between cure degrees with CNT presence can be attributed to higher thermal conductivity of samples constituted by CNTs. Thus, the heat spreads quickly in the particles of the composites, and the cure degree achieved is greater than in the neat resin. Puglia et al.[37] also showed that the extent of cure reaction for samples constituted by DGEBA, diethylenetriamine and SWCNT cured isothermally at 40°C was higher than those obtained from same samples without the addition of SWCNT.

Figure 12 also shows that, until about 50 min, sample ResCNT-Ac showed slightly higher degree of cure than the other composites. This elevated reaction rate at the beginning of the reaction for sample ResCNT-Ac may be related to the presence of hydroxyl groups (—OH) on the surface of the CNTs, which has a catalytic effect on epoxy ring opening, as proposed by Xie et al.[38] They showed[38] that, after the higher initial reaction rate of the acid-CNTs/epoxy composite compared to the neat resin, the last stage of the cure remained unaffected by CNTs.

Figures 11 and 12 also show that each CNT treatment caused differences in the cure degree curves. The rates of cure degree of the samples ResCNT-Ac and ResCNT-An are considerably higher at the beginning of the reaction. Meanwhile, the cure degree of the samples ResCNT-0 and ResCNT-Am increases in a more gradual and smooth way with extension of the reaction. The homogeneity and dispersion of nanotubes in the matrix may influence the cure rate of the resin. Samples ResCNT-An

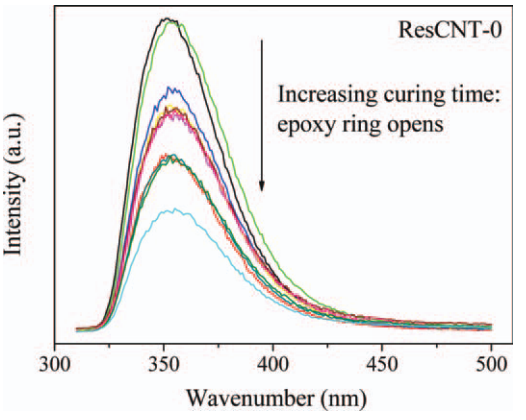

Figure 10. Emission spectra (λ_{ex}= 300, luminescence spectroscopy) for sample ResCNT-0 precured at 80°C for 1 hour and them cured at 120°C for different times between 0 and 18 hours. [Color figure can be viewed in the online issue, which is available at wileyonlinelibrary.com.]

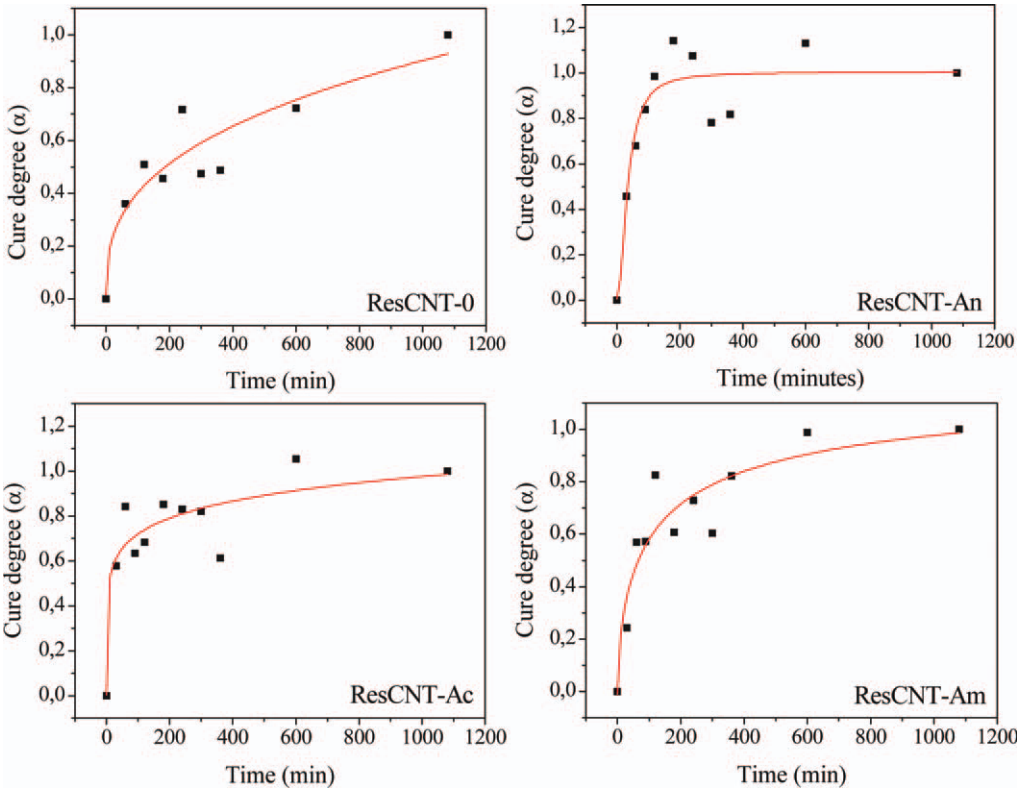

Figure 11. Cure degree for samples ResCNT-0, ResCNT-An, ResCNT-Ac, and ResCNT-Am, using emission spectra (luminescence spectroscopy); squares: experimental points obtained from eq. (1), lines: fitting of the data obtained from eq. (1). [Color figure can be viewed in the online issue, which is available at wileyonlinelibrary.com.]

and ResCNT-Ac, the less homogeneous as shown by the micrographs of Figure 8, showed greater cure degree rate at the beginning of the reaction. Besides that, the composite ResCNT-An was the less homogeneous one, and this sample showed the highest values of cure degree throughout the reaction. However, samples ResCNT-0 and ResCNT-Am, the most homogeneous ones, showed a smooth cure degree curve throughout the reaction. The good dispersion of amine-functionalizated CNTs in epoxy resin may be related to the fact that the curing reaction of this sample did not occur with great intensity at any stage of the reaction, but more gradually, as occurred with sample ResCNT-Am and ResCNT-0.

The results obtained from luminescence spectroscopy for samples cured at 120°C for 2 h (after the precuring at 80°C for 1 h) are consistent with those obtained by Raman spectroscopy for the same samples submitted to the same cure cycle. However, the direct comparison between the Raman results of a same sample cured at 80 and 120°C is a complicated task due to the different background (luminescence) effects in the Raman spectra. This Raman luminescence effect depends on the time and temperature of cure. Nevertheless, the luminescence spectroscopy was effective to compare the properties of both samples.

Finally, it should be noted that many published studies did not show much difference between the values of cure degree and the curing rate between neat epoxy resin and epoxy resin/CNT nanocomposites. Nevertheless, none of these works studied the cure process by luminescence spectroscopy, which is a very sensitive analysis, and thus, it can better distinguish the difference between the curves of cure degree of neat resin and nanocomposites.

CONCLUSIONS

CNTs were successfully functionalized by acid and amine treatments and the presence of these functional groups were confirmed by infrared spectra (FTIR).

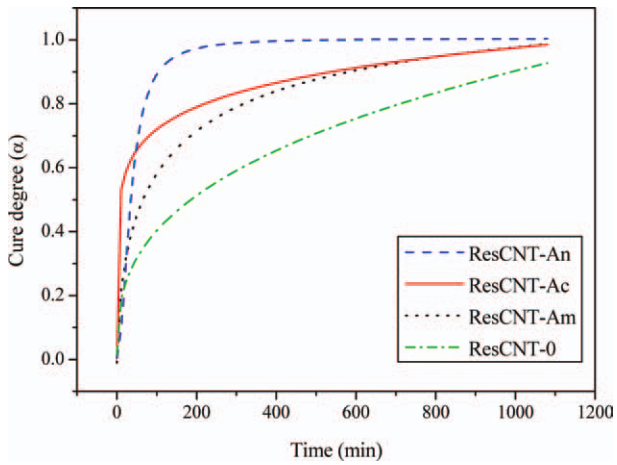

Figure 12. Cure degree for samples ResCNT-0, ResCNT-An, ResCNT-Ac, and ResCNT-Am. using emission spectra [fitting of the data obtained from eq. (1)]. [Color figure can be viewed in the online issue, which is available at wileyonlinelibrary.com.]

EDS, TGA curves, and Raman spectroscopy showed that annealing procedure followed by acid treatment was effective for CNT purification, without damaging its crystal structure.

Micrographs showed that amine-functionalized CNTs have more disorganized microstructures, which lead to greater dispersion of CNTs.

The nanocomposites synthesized with annealed CNTs and acid-treated CNTs showed the presence of agglomerates, unlike the nanocomposites synthesized with amine-functionalized nanotubes, which was the most homogeneous of all and had the better interfacial bonding between CNT and resin.

Raman and luminescence spectroscopy showed a good correlation of results to study the cure of epoxy resin and nanocomposites for a same time/temperature. Although it was not possible to compare Raman spectra of samples cured for different times (because of luminescence activities), this was possible with the luminescence spectra.

In a general way, the presence of CNTs, functionalized or not, increased the cure degree of the samples. This must occur due to the thermal conductivity of CNTs, which increases the heat diffusion in the samples, increasing the cure degree of the composites. At the early stages of cure reaction, composites prepared with annealed CNTs and acid-treated CNTs showed the highest cure degree rates. The initial acceleration of cure should be related to the presence of CNT agglomerates in these composites, and to the presence of hydroxyl groups in acid CNTs.

ACKNOWLEDGMENTS

The authors gratefully acknowledge FAPESP for financial support and LAS/INPE and UNIVAP for collaboration.

REFERENCES

1. Ooi, S. K.; Cook, W. D.; Simona, G. P.; Suchb, C. H. *Polymer* **2000,** *41*, 3639.
2. Chen, H.; Jacobs, O.; Wu, W.; Rüdiger, G.; Schuädel, B. *Polym. Test* **2007,** *26*, 351.
3. Puglia, D.; Valentini, L.; Armentano, I.; Kenny, J. M. *Diamond Relat. Mater.* **2003,** *12*, 827.
4. Tao, K.; Yang, S.; Grunlan, J.C.; Kim, Y.S.; Dang, B.; Deng, Y.; Thomas, R.L.; Wilson, B.L.; Wei, X. *J. Appl. Polym. Sci.* **2006,** *102*, 5248.
5. Sahoo, N. G.; Rana, S.; Cho, J. W.; Li, L.; Chan, S. H. *Prog. Polym. Sci.* **2010,** *35*, 837.
6. Shen, J.; Huang, W.; Wu, L.; Hu, Y.; Ye, M. *Compos. Sci. Technol.* **2007,** *67*, 3041.
7. Meng, H.; Sui, G. X.; Fang, P. F.; Yang, R. *Polymer* **2008,** *49*, 610.
8. Ma, P. C.; Mo, S. Y.; Tang, B. Z.; Kim, J. K. *Carbon* **2010,** *48*, 1824.
9. Wang, S.; Liang, Z.; Liu, T.; Wang, B.; Zhang, C. *Nanotechnology* **2006,** *17*, 1551.
10. Shen, J.; Huang, W.; Wu, L.; Hu, Y.; Ye, M. *Composites A* **2007,** *38*, 1331.
11. Callister, W. D., Jr, Ciência de Engenharia de Materiais: Uma Introdução; LTC: Rio de Janeiro, **2002.**
12. Loos, M. R.; Coelho, L. A. F.; Pezzin, S. H; Amico, S. C. *Mater. Res.* **2008,** *11*, 347.
13. Oriakhi, C. O. *J. Chem. Educ.* **2000,** *77*, 1138.
14. Baughman, R. H.; Zakhidov, A. A.; Heer, W. A. *Science* **2002,** *297*, 787.
15. Catalani, A.; Bonicelli, M. G. *Thermochim. Acta* **2005,** *438*, 126.
16. Yang, K.; Gu, M.; Jin, Y. *J. Appl. Polym. Sci.* **2008,** *110*, 2980.
17. Abdalla, M.; Dean, D.; Robinson, P.; Nyairo, E. *Polymer* **2008,** *49*, 3310.
18. Zhengping, F.; Jianguo, W.; Aijuan, G.; Lifang, T. *Front. Mater. Sci. China* **2007,** *1*, 415.
19. Pozuelo, J.; Baselga, J. *J. Mater. Process. Technol.* **2003,** *143*, 332.
20. Torkelson, J. M.; Quirin, J. C. *Polymer* **2003,** *44*, 423.
21. Huang, W.; Wang, Y.; Luo, G.; Wei, F. *Carbon* **2003,** *41*, 2585.
22. Antunes, E. F.; Resende, V. G.; Mengui, U. A.; Cunha, J. B. M.; Corat, E. J.; Massi, M. *Appl. Surf. Sci.* **2011,** *257*, 8038.
23. Yuen, S. M.; Ma, C. C. M.; Lin, Y. Y.; Kuan, H. C. *Compos. Sci. Technol.* **2007,** *67*, 2564.
24. Vuković, G. D.; Marinković, A. D.; Colić, M.; Ristić, M. D.; Aleksić, R.; Perić-Grujić, A. A.; Uskokovic, P.S. *Chem. Eng. J.* **2010,** *157*, 238.
25. Li, J.; Tang, T.; Zhang, X.; Li, S.; Li, M. *Mater. Lett.* **2007,** *61*, 4351.
26. Ramanathan, T.; Fisher, F. T.; Ruoff, R. S.; Brinson, L. C. *Chem. Mater.* **2005,** *17*, 1290.
27. Xiong, J.; Zheng, Z.; Qin, X.; Li, M.; Li, H.; Wang, X. *Carbon* **2006,** *44*, 2701.
28. Awasthi, K.; Singh, D. P.; Singh, S. K.; Dash, D.; Srivastava, O. N. *New Carbon Mater.* **2009,** *24*, 301.
29. Liu, L.; Qin, Y.; Guo, Z. X.; Zhu, D. *Carbon* **2003,** *41*, 331.
30. Yang, L.; Chen, J.; Wei, X.; Liu, B.; Kuang, Y. *Electrochim. Acta* **2007,** *53*, 777.
31. Kuan, H. -C.; Ma, C. -C. M.; Chan, W. -P.; Yuen, S. -M.; Wu, H. -H.; Lee, T. -M. *Compos. Sci. Technol.* **2005,** *65*, 1703.
32. Wang, Z.; Huang, X.; Xue, R.; Chen, L. *J. Appl. Phys.* **1998,** *84*, 227.
33. Belin, T.; Epron, F. *Mater. Sci. Eng. B* **2005,** *119*, 105.
34. Yang, S. -Y.; Ma, C. -C. M.; Teng, C. -C.; Huang, Y. -W.; Liao, S. -H.; Huang, Y. L.; Tien, H.-W.; Lee, T.-M.; Chiou, K.-C. *Carbon* **2010,** *48*, 592.
35. Chike, K. E.; Myrick, M. L.; Lyon, R. E.; Angels, S. M. *Appl. Spectroc.* **1993,** *47*, 1631.
36. Silveira, J. B. Preparação e caracterização de resina epóxi transparente dopada com nanoestruturas semicondutoras de CdS. 115f. **2009.** Thesis (Master of Materials Science), Universidade Estadual Paulista, Ilha Solteira.
37. Puglia, D.; Valentini, L.; Kenny, J. M. *J. Appl. Polym. Sci.* **2003,** *88*, 452.
38. Xie, H.; Liu, B.; Yuan, Z.; Shen, J.; Cheng, R. *J. Polym. Sci. Part B: Polym. Phys.* **2004,** *42*, 3701.